HHS Public Access

Author manuscript

Bone. Author manuscript; available in PMC 2021 July 01.

Published in final edited form as:

Bone. 2020 July ; 136: 115369. doi:10.1016/j.bone.2020.115369.

Increasing Fluoride Content Deteriorates Rat Bone Mechanical Properties

Taraneh Rezaee[a], **Mary L. Bouxsein**[b], **Lamya Karim**[a]

[a]Department of Bioengineering, University of Massachusetts Dartmouth, 285 Old Westport Road, Dartmouth, MA 02747, USA

[b]Center for Advanced Orthopedic Studies, Beth Israel Deaconess Medical Center, 330 Brookline Avenue, Boston, MA 02115

Abstract

Elevation of bone fluoride levels due to drinking beverages with high fluoride content or other means such as inhalation can result in skeletal fluorosis and lead to increased joint pain, skeletal deformities, and fracture. Because skeletal fluorosis alters bone's mineral composition, it is likely to affect bone's tissue-level mechanical properties with consequent effects on whole bone mechanical behavior. To investigate this, we determined whether incubation with *in vitro* sodium fluoride (NaF) altered bone's mechanical behavior at both the tissue- and whole bone-levels using cyclic reference point indentation (cRPI) and traditional 3-point bending, respectively. Forty-two ulnas from female adult rats (5–6 months) were randomly divided into 5 groups (vehicle, 0.05M NaF, 0.25M NaF, 0.75M NaF, and 1.5M NaF). Bones were washed in a detergent solution to remove organic barriers to ion exchange and incubated in respective treatment solutions (12hrs, 23°C). Cortical tissue mineral density (TMD) and geometry at the mid-diaphysis were determined by microCT. cRPI was performed on the distal diaphysis (9N, 2Hz, 10 cycles), and then bones were tested in 3-point bending to assess whole bone mechanical properties. The incubations in vehicle (0M) up to 1.5M *in vitro* NaF concentrations achieved bone fluoride levels ranging from approximately 0.70 to 15.8 ppm. NaF-incubated bones had significantly greater indentation distances, higher displacement-to-maximum force, and lower estimated elastic modulus, ultimate stress, and bending rigidity with increasing NaF concentration compared to vehicle-incubated bones. cRPI variables were moderately correlated to whole bone mechanical properties such that higher indentation distances were associated with lower estimated elastic modulus, ultimate stress, and bending rigidity. In conclusion, *in vitro* NaF incubation mostly has a deleterious effect on

Corresponding author: Lamya Karim, University of Massachusetts Dartmouth, Department of Bioengineering, 285 Old Westport Road, TEX 214, Dartmouth, MA 02740, Phone: 508-999-8560, lkarim@umassd.edu.

Credit Author Statement

Taraneh Rezaee: data curation, formal analysis, investigation, visualization, writing – original draft, writing – review & editing; **Mary Bouxsein**: conceptualization, methodology, project administration, resources, supervision, writing – original draft, writing – review & editing; **Lamya Karim**: conceptualization, data curation, formal analysis, funding acquisition, investigation, methodology, project administration, resources, supervision, validation, visualization, writing – original draft, writing – review & editing

bone mechanical behavior with increasing NaF levels that is independent of bone turnover and reflected, in part, by less resistance of the tissue to cRPI-based indentation.

Keywords

Sodium fluoride; skeletal fluorosis; mechanical properties; reference point indentation; bone

1. Introduction

Skeletal fluorosis (SF) is a debilitating bone disease that affects millions of people worldwide specifically populations in south and east Asia (e.g., India, China, Japan), Africa, the Middle East, Argentina, and Australia [1, 2]. SF typically arises due to prolonged consumption of drinking tea or well water with fluoride concentration (F^-) over 4 parts per million (ppm), although instances of SF have been identified in patients with exposure to F^- levels below 4 ppm as well [3–6]. The World Health Organization has stated that the maximum safe limit of fluoride in drinking water is 1.5 ppm [7]. As a result of high fluoride ingestion, there is an excessive accumulation of fluoride in bone, which can disturb the delicate balance in bone turnover processes and consequently result in joint pain, muscle weakness, development of osteophytes, and other debilitating skeletal deformities [8–10]. Research has focused on treatment with vitamin D, vitamin C, and calcium to remedy SF, but these approaches have shown minimal efficacy [11]. Currently, the only method available to treat SF is to eliminate exposure to fluoride [12], which is a major challenge in geographical areas with high levels of fluoride exposure in water, tea, and volcanic rock in the environment. Therefore, it is important to improve our understanding of the effects of fluoride on the behavior of skeletal tissue in order to emphasize the necessity for clean drinking water worldwide and develop better treatments for those suffering from extreme fluoride exposure.

It is generally understood that fluoride exposure increases bone fracture incidence. Specifically, clinical trials using fluoride therapy for patients suffering from osteoporosis have shown that fluoride administration increases fracture rates and/or significantly reduces bone strength at the vertebra, iliac crest, and other skeletal sites [13–18]. It is also known that SF alters the bone formation process by activating osteoblasts in early stages to proliferate and lay down immature woven bone [19], which has a weaker collagen pattern than mature lamellar bone and may be a reason for the observed reductions in bone strength. However, very little is known about skeletal pathology and mechanical behavior due to SF at the micro- and nano-scale. A few studies have tested whole bone mechanical properties in animals provided extreme levels of fluoridated drinking water [20–22] and in murine bone subjected to a single concentration of in vitro sodium fluoride incubation [23]. However, none of these studies have assessed tissue-level mechanical properties at the micro-scale. Other studies investigating the effects of fluoride on bone have focused primarily on how fluoride treatment affects mineralization in bone but few have assessed mechanical properties [24–27].

Thus, we aimed to investigate how increased fluoride content affects bone mechanical properties. Among the factors that can affect whole bone mechanical behavior are bone density, geometry, microarchitecture, and inherent tissue mechanical properties [28]. Although the influences of bone geometry and microarchitecture on whole bone strength and fracture risk are well documented, the contribution of bone tissue material properties is less well understood [29, 30]. A few investigations have been conducted to explore the effect of changes in bone tissue material properties on whole bone strength [30–33], but the exact nature of how nano- and micro-scale factors affect fracture resistance is still unclear. Additional investigations are needed to address whether mechanisms acting at the nano- or microscale in bone tissue influence whole bone mechanical behavior. Furthermore, assessment of some aspects of bone tissue material properties is now possible by cyclic reference point indentation (cRPI). cRPI is a type of microindentation, but does not require special surface preparation like traditional microindentation methods and measures the indentation distance traveled into the bone by a test probe relative to a reference probe on the bone surface over a number of cycles [34–41].

Importantly, to assess the effects of fluoride exposure, bone specimens can be altered with sodium fluoride (NaF) using an established technique in which bone specimens are incubated *in vitro* [42, 43]. NaF incubation leads to altered matrix mineralization and mineral crystal size due to substitution of the hydroxyl group of hydroxyapatite by fluoride [44, 45]. A few studies have shown that NaF incubation, which alters the physico-chemical structure of bone mineral [44–46], leads to increased bone mass, but worse bone strength and increased fracture incidence [47].

We aimed to understand how NaF affects bone mechanical properties at different length scales and provide further insight on how cRPI measurements relate to traditional mechanical properties. Here, we used cRPI and traditional 3-point bending to assess bone indentation properties and whole bone mechanical properties, respectively, in rat bone specimens that were subjected to *in vitro* NaF incubations to induce alterations to bone mineral. We hypothesized that *in vitro* NaF incubation would lead to deteriorated cortical bone indentation properties and whole bone mechanical properties with increasing NaF levels.

2. Methods

2.1. Specimen collection

Forty-two ulnae, which have a relatively straight geometry and are ideal for mechanical testing, were dissected from 21 female Fisher rats (5–6 months old). Ulnas were randomly divided into 5 groups: vehicle (VEH, n=8), 0.05M NaF (n=9), 0.25M NaF (n=8), 0.75M NaF (n=9), and 1.5M NaF (n=8).

2.2. In vitro sodium fluoride incubation

Bone specimens were incubated *in vitro* in NaF based on an established protocol used in whole rodent bone [23]. Bones were washed for 24 hours in a detergent solution (0.1% Tergitol NP-40) to remove any organic barriers to ion exchange before NaF incubations. The

bones were then incubated for 12 hours at room temperature with constant agitation in their respective incubation solutions. Incubation solutions consisted of phosphate buffered saline and calcium chloride (45 mg/L) with the corresponding molarity of NaF added to each group. Bones were then stored at −20°C in saline soaked gauze until further use.

2.3. Assessment of cortical geometry and tissue mineral density

After incubations were complete, each ulna was scanned at the mid-diaphysis (at 50% of the total length) using microcomputed tomography (microCT 40, Scanco Medical AG, Brüttisellen, Switzerland) at 12 microns voxel resolution, 70 kVP x-ray tube potential, 114 uA x-ray intensity, and 200 ms integration time to determine bone's geometry (e.g. Imax [mm^4], Imin [mm^4]), cortical thickness [mm], cortical porosity [%], and tissue mineral density [mgHA/ccm]. 204 slices were acquired, reconstructed overnight, fitted with a contour around the periosteal surface of midshaft, and segmented using a threshold of 0.71 g/cm^3 HA.

2.4. Assessment of cortical tissue properties via cyclic reference point indentation (cRPI)

The cyclic reference point indentation system (Biodent 1000 Hfc, Active Life Scientific, Santa Barbara, CA, USA) equipped with BP2 test probes with a 90° 2.5 μm cono-spherical shaped tip (Active Life Scientific, Santa Barbara, CA) was used to indent each ulna while hydrated on the posterior surface of the distal diaphysis at a maximum force of 9 N at 2 Hz for 10 cycles. The following variables were determined: indentation distance (ID, indentation distance measured in the first cycle [μm]), creep indentation distance (CID, total indentation distance during the hold step of the first cycle [μm]), average creep indentation distance (avg CID [μm]), total indentation distance (TID, total indentation distance across all cycles [μm]), indentation distance increase (IDI, increase in the indentation distance in the last cycle relative to that in the first cycle [μm]), average energy dissipation (avg ED, area enclosed by the test's hysteresis loop from the third to last cycle [μJ]), average unloading slope (avg US, average unloading slope from third to last cycle [N/μm]), and average loading slope (avg LS, average loading slope from third to last cycle [N/μm]). For each bone, 3 indentation measurements were taken and averaged, and all 3 indentations were made outside of the region of 3-point bending tests.

2.5. Assessment of whole bone mechanical properties via 3-point bending

Ulnas were then tested in 3-point bending while hydrated using a micromechanical testing system (ElectroForce 3230; Bose Corporation, Framingham, MA) with WinTest 4.1 software. Specimens were cleaned of all soft tissue and placed in a 3-point bending configuration with a span length of 18 mm. A preload of 0.4 N was applied, and then a loading rate of 0.03 mm/s was applied to the bone until failure. A custom made MATLAB script was utilized to calculate the following parameters from the force-deformation data: ultimate moment (Nmm), ultimate stress (N/mm^2), estimated elastic modulus (GPa), displacement-to-maximum (mm), work-to-ultimate point (Nmm), and bending rigidity (Nmm^2).

2.6. Assessment of fluoride concentration

Fluoride concentration was measured to confirm the amount of fluoride uptake due to *in vitro* incubation. A portion (mass = 4.65 ± 1.21 mg) of each incubated and mechanically tested bone specimen was ashed at 550°C for 18 hrs. The ashed bone samples were then dissolved in 1mL 0.25M HCl, and the excess acid was neutralized with 0.125M NaOH. The solution volume was brought up to 5mL using deionized water. Bone fluoride content (ppm) relative to a fluoride standard curve was determined using a fluoride ion-selective probe (Thermo Scientific, Orion-9609BNWP).

2.7. Statistical analyses

Shapiro-Wilk analysis was used to determine normality for all variables. Majority of the variables were normally distributed except for a few (e.g. bending rigidity). Spearman correlation analyses were used to determine associations between variables. ANOVA with Dunnet post-hoc tests were used to determine differences between NaF-incubated groups and the vehicle control group for cortical tissue mineral density, cortical geometry properties, cRPI variables, whole-bone mechanical variables, and fluoride concentration. For variables that were not normally distributed (e.g. bending rigidity), Kruskal-Wallis tests were used to identify differences between groups; these tests showed the same results as ANOVA tests, which are reported in the text and tables. The Wilcoxon trend test was used to determine whether there were any trends in measured variables with increasing NaF concentration.

3. Results

Measured fluoride content was higher in specimens incubated *in vitro* in higher NaF concentrations ($p \leq 0.05$, Figure 1, Table 1), and Wilcoxon trend tests showed that there was a significant trend between NaF concentration and fluoride ($p \leq 0.05$). ID, IDI, CID, avg CID, and TID (measurements of indentation distance into the bone) and avg ED (amount of energy dissipated) all increased whereas avg LS and avg US (material stiffness during loading and unloading, respectively) decreased with increasing NaF concentration (Table 1), and Wilcoxon trend tests showed that there were significant trends between NaF concentration and all cRPI variables ($p \leq 0.05$). All NaF-incubated groups had greater indentation distance measures and increased avg ED than vehicle-incubated bones ($p \leq 0.05$, Figure 2). For avg LS, the 0.75M and 1.5M groups were significantly lower than vehicle controls. Although avg US followed the same trend, none of the NaF-incubated groups were significantly different from controls. Apparent elastic modulus, ultimate moment, and ultimate stress decreased while displacement-to-maximum load increased with increasing NaF concentration (Table 1, Figure 3), and Wilcoxon trend tests showed that there were significant trends between amount of NaF concentration and these mechanical testing variables ($p \leq 0.05$). Bending rigidity was also lower with increasing NaF concentrations compared to the vehicle group ($p \leq 0.05$) (Table 1).

Fluoride content was positively correlated with IDI ($r = +0.62$, $p \leq 0.05$), ID ($r = +0.51$, $p \leq 0.05$), TID ($r = +0.53$ $p \leq 0.05$), and CID ($r = +0.52$, $p \leq 0.05$) measured by cRPI, and with some but not all 3-point bending variables (i.e. displacement-to-maximum force ($r = +0.60$,

p≤0.05), work-to-ultimate point (r = +0.30, p≤0.05)) (Table 2). Fluoride concentration was negatively correlated with cortical TMD as assessed by microCT (r = −0.30, p≤0.05), with loading slope assessed by cRPI (r = −0.56, p≤0.05), and with several 3-point bending properties (i.e. elastic modulus (−0.62, p≤0.05), ultimate moment (r = −0.59, p≤0.05), ultimate stress (r = −0.60, p≤0.05), and bending rigidity (r = −0.59, p≤0.05)) (Table 2). Fluoride content, however, was not associated with I_{max}, I_{min}, cortical thickness, cortical porosity, or cRPI-assessed unloading slope (Table 2).

Cortical TMD was negatively associated with both IDI and CID, and its relationship with the other indentation distances trended in the same direction. Cortical TMD was negatively correlated with average ED and positively correlated with both average US and average LS. Cortical porosity was positively associated with indentation distances and average ED, and negatively associated with average LS. Cortical thickness was not significantly associated with any cRPI variables. Spearman correlation coefficients between cRPI variables and microCT properties are summarized in Table 2.

ID, IDI, CID, avg CID, TID, and average ED were negatively correlated with apparent elastic modulus, ultimate moment, ultimate stress, and bending rigidity, but positively correlated with displacement-to-maximum force and work-to-ultimate point (Table 2). Average LS was positively correlated with estimated elastic modulus, ultimate moment, and bending rigidity, but was negatively correlated with displacement-to-maximum force (Table 2). Average US was positively correlated with estimated elastic modulus, but had no significant correlations with other whole bone mechanical properties (Table 2).

4. Discussion

Skeletal fluorosis (SF), which is generally caused by consumption of well water or tea containing fluoride concentrations in excess of 4 parts per million (ppm) [2], is known to cause bone lesions and joint pain [11, 48]. However, little data is available on how it affects bone's tissue level mechanical properties. cRPI is a relatively new method designed to evaluate the intrinsic tissue mechanical properties of cortical bone. To date, there are few data showing the sensitivity of this technique to changes in bone's extracellular matrix. We induced changes in rat bone matrix using controlled *in vitro* incubation with NaF that alters the bone mineral with fluoride. Our primary goal was to study the effect of *in vitro* NaF incubation on bone mechanical properties, as assessed by whole bone and tissue-level mechanical testing.

We aimed to determine whether cRPI can detect changes in rat cortical bone tissue induced by *in vitro* NaF incubation at various concentrations. We found that *in vitro* exposure to increased concentrations of NaF led to deteriorated cortical bone tissue-level mechanical properties. Specifically, NaF incubation led to greater indentation distances, indicating that the bone tissue was less resistant to a fracture in the cortex induced by a cono-spherical tip. We assessed fluoride content in bone specimens to confirm the amount of fluoride uptake due to *in vitro* incubation. The bone fluoride measurements confirmed that increased bone fluoride content was associated with increased indentation distances by cRPI. The observation of increased indentation distances with increased NaF concentrations supports

findings in another study that, although did not investigate skeletal fluorosis, showed a positive association between increased matrix mineralization and cRPI indentation distances [49]. Moreover, *in vitro* incubation in fluoride results in the hydroxyapatite being converted to a fluoroapatite, which alters the structure and overall stability of the mineral crystal [23, 50, 51]. Consequently, the deeper indentation distances may result from the NaF induced altered mineralization, which can deteriorate whole bone mechanical properties. In support of this contention, our bending results showed that NaF-incubated bones had a lower estimated elastic modulus, bending rigidity, and ultimate stress compared to vehicle controls, and this was reinforced by the measurements of fluoride content.

Our results support several previous studies in animal models that indicated there was decreased elastic modulus and fracture load in femurs of growing rats treated with fluoride [20], decreased bending strength in sheep with high fluoride exposure in drinking water [21], and decreased femoral strength in rabbits that drank fluoridated water [22]. Studies in human bone also similarly showed that cortical bone had lower elastic modulus in SF tissue compared to healthy bone specimens [52, 53]. Additionally, several human studies indicated increased prevalence of skeletal deformities or higher hip fracture risk in those who consume fluoridated water or live in areas of high fluoride levels in the environment [54–63]. Only two of the aforementioned animal studies directly measured fluoride in bone specimens with F^- levels ranging 620 – 8,150 ppm [20] and 1,151 – 7,893 ppm [22]. Both studies report extreme levels of bone fluoride content resulting from SF due to drinking fluoridated water with extremely high levels of fluoride (16 ppm [20] and 100 ppm [22], respectively) compared to the 1.5 ppm safe limit for fluoride in water as indicated by the World Health Organization [7]. Among the abovementioned human studies, one measured bone fluoride content ranging from 2,042 – 10,142 ppm in the ilium and rib from anthropologic specimens found in areas of extremely high environmental fluoride levels due to volcanic activity [58]. Our fluoride measurements were on the order of 1000x lower (ranging from ~2.36—15.8 ppm) than in these previous reports in fluorotic bone. Despite having much lower overall fluoride levels, our findings still show that increased fluoride content can deteriorate whole bone mechanical properties. However, future work is still needed to determine the distribution of fluoride content across different bones and to understand how our *in vitro* results may compare to bone alterations due to skeletal fluorosis resulting from direct ingestion of fluoride. Our findings regarding estimated elastic modulus were in contrast to a previous study conducted in ovariectomized rats that reported increased elastic modulus in the femur due to in vivo treatment with fluoridated drinking water [64]. There were a number of differences between these studies, including in vitro treatment of ulnae from young healthy rats versus in vivo treatment in old osteopenic rats. We were unable to make any additional comparisons because bone fluoride content was not reported in the study by Giaveresi, et al. Further investigation is required to better understand these differences.

In addition to the trends observed in *in vivo* studies, our results are also similar to previous findings conducted in murine femurs subjected to *in vitro* incubation that showed *in vitro* 1.5M NaF incubation resulted in reduced ultimate load and rigidity but increased deformation-to-failure (indicating a more ductile material) [23]. Another *in vitro* study conducted on bovine femoral cortical bone specimens also similarly showed that NaF-incubated specimens had lower elastic modulus, yield and ultimate stress, and hardness, and

that these effects increased with increasing NaF concentration (0.145 M, 0.5 M, and 2.0 M) [46]. Thus, our findings regarding how increased bone fluoride content relate to bone mechanical properties are consistent with trends from reports utilizing both *in vivo* (i.e., drinking fluoride-treated water) and *in vitro* (i.e., incubating bone in fluoride) methods.

We also assessed the relationships between cRPI measures and cortical tissue mineral density and morphology. cRPI-assessed indentation distances were negatively correlated with cortical TMD (r^2 = 9% to 10%), positively associated with cortical porosity (r^2 = 10% to 12%), and not associated with cortical thickness. Thus, it is implied that less mineralized and more porous bone has less resistance to indentation, resulting in the observed larger indentation distances. However, the relationships were very weak, and these findings are similar to results in our recent study conducted on human cadaveric bone in which we observed very weak relationships between cortical geometry and cRPI variables [65]. Our results suggest that cRPI measurements are not, or are only very minimally, influenced by cortical microarchitecture.

Further, we investigated the relationship between cRPI variables and traditional mechanical properties. A few cRPI studies have been conducted that assessed relationships between cRPI variables and traditional mechanical properties. For example, experiments done in dog, rat, and human bone showed that there are negative relationships between IDI and toughness assessed from bending tests, suggesting that increased indentation distances are indicative of bone with deteriorated mechanical integrity [39, 66]. Our results support this concept as we identified moderate associations between cRPI measures and whole bone mechanical properties assessed by 3-point bending. Specifically, deteriorated whole bone mechanical properties (e.g. lower estimated elastic modulus, lower bending rigidity) was associated with lower loading (r^2 = 17% to 28%) and unloading (r^2 = 10%) slopes and increased indentation distances (r^2 = 25% to 53%). We observed these relationships even with our cRPI measures having much lower variation compared to previous studies. With the various concentrations of NaF incubation, we observed that IDI measures ranged from 7.2 to 12.0 μm. In comparison, a study by Gallant, *et al.* reported an almost 3-fold IDI range from ~6.0 to 16.5 μm and a study by Diez-Perez, *et al.* observed an even wider range with IDI values ranging from ~9.9 to 27.4 μm [37]. However, these studies used data from a combination of several animal models pooled together or from humans with a skewed age group (4 young donors, 1 old donor), respectively.

In conclusion, our results illustrate that cRPI measurements can detect alterations in cortical bone tissue due to *in vitro* NaF incubations. Specifically, we found that the NaF incubation resulted in deteriorated tissue indentation properties, corresponding to detrimental effects on its overall mechanical integrity. This study lends support to the idea that cRPI may serve as a useful tool to measure material properties of bone in which the mineral matrix is altered. Thus, insights from this study will be useful in design of future studies aiming to identify underlying mechanisms of skeletal fragility due to SF. However, further work must first be done to confirm our findings from a rat model in healthy human bone and in bone from patients with SF to understand mechanical changes of the skeletal system due to excessive fluoride accumulation.

Acknowledgements

We thank Mamadou Diallo for his help with microCT scanning and *in vitro* incubations, and Tianna Edwards and Richard Bender for their help with measurement of fluoride. Funding for this work was provided by the National Institute on Aging training grant T32AG023480. Dr. Karim is currently supported by the National Institute of Arthritis and Musculoskeletal and Skin Diseases under award number K01AR069685. The content is solely the responsibility of the authors and does not necessarily represent the official views of the funding agencies.

References

[1]. Tucci JR, Whitford GM, McAlister WH, Novack DV, Mumm S, Keaveny TM, Whyte MP, Skeletal Fluorosis Due To Inhalation Abuse of a Difluoroethane- Containing Computer Cleaner, J Bone Miner Res 32(1) (2017) 188–195. [PubMed: 27449958]

[2]. Whyte MP, Essmyer K, Gannon FH, Reinus WR, Skeletal fluorosis and instant tea, Am J Med 118(1) (2005) 78–82. [PubMed: 15639213]

[3]. Choubisa S, Fluorosis in some tribal villages of Udaipur district (Rajasthan), J Environ Biol 19(4) (1998) 341–352.

[4]. Choubisa S, Some observations on endemic fluorosis in domestic animals in Southern Rajasthan (India), Vet Res Comm 23(7) (1999) 457–465.

[5]. Roy S, Dass G, Fluoride contamination in drinking water–a review, Resour Environ 3(3) (2013) 53–58.

[6]. Whyte MP, Totty WG, Lim VT, Whitford GM, Skeletal fluorosis from instant tea, J Bone Miner Res 23(5) (2008) 759–769. [PubMed: 18179362]

[7]. Gupta N, Gupta N, Chhabra P, Image diagnosis: dental and skeletal fluorosis, Perm J 20(1) (2016) e105. [PubMed: 26824971]

[8]. Hewavithana P, Jayawardhane W, Gamage R, Goonaratna C, Skeletal fluorosis in Vavuniya District: an observational study, Ceylon Med 63(3) (2018).

[9]. Fawell J, Bailey K, Chilton J, Dahi E, Magara Y, Fluoride in drinking-water, IW publishing 2006.

[10]. Oweis R, Associations between fluoride intakes, bone outcomes and dental fluorosis, University of Iowa (2018).

[11]. Chen Y, Yan W, Hui X, Treatment and prevention of skeletal fluorosis, Biomed Environ Sci 30(2) (2017) 147–149. [PubMed: 28292354]

[12]. Fabreau GE, Bauman P, Coakley AL, Johnston K, Kennel KA, Gifford JL, Sadrzadeh HM, Whitford GM, Whyte MP, Kline GA, Skeletal fluorosis in a resettled refugee from Kakuma refugee camp, Lancet 393(10168) (2019) 223–225. [PubMed: 30663587]

[13]. Gutteridge DH, Stewart GO, Prince RL, Price RI, Retallack RW, Dhaliwal SS, Stuckey BG, Drury P, Jones CE, Faulkner DL, Kent GN, Bhagat CI, Nicholson GC, Jamrozik K, A randomized trial of sodium fluoride (60 mg) +/− estrogen in postmenopausal osteoporotic vertebral fractures: increased vertebral fractures and peripheral bone loss with sodium fluoride; concurrent estrogen prevents peripheral loss, but not vertebral fractures, Osteoporos Int 13(2) (2002) 158–70. [PubMed: 11908491]

[14]. Haguenauer D, Welch V, Shea B, Tugwell P, Adachi JD, Wells G, Fluoride for the treatment of postmenopausal osteoporotic fractures: a meta-analysis, Osteoporos Int 11(9) (2000) 727–38. [PubMed: 11148800]

[15]. Sogaard CH, Mosekilde L, Richards A, Mosekilde L, Marked decrease in trabecular bone quality after five years of sodium fluoride therapy--assessed by biomechanical testing of iliac crest bone biopsies in osteoporotic patients, Bone 15(4) (1994) 393–9. [PubMed: 7917577]

[16]. Schnitzler CM, Wing JR, Gear KA, Robson HJ, Bone fragility of the peripheral skeleton during fluoride therapy for osteoporosis, Clin Orthop Relat Res (261) (1990) 268–75.

[17]. Riggs BL, Hodgson SF, O'Fallon WM, Chao EY, Wahner HW, Muhs JM, Cedel SL, Melton LJ 3rd, Effect of fluoride treatment on the fracture rate in postmenopausal women with osteoporosis, N Engl J Med 322(12) (1990) 802–9. [PubMed: 2407957]

[18]. Bayley TA, Harrison JE, Murray TM, Josse RG, Sturtridge W, Pritzker KP, Strauss A, Vieth R, Goodwin S, Fluoride-induced fractures: relation to osteogenic effect, J Bone Miner Res 5 Suppl 1 (1990) S217–22. [PubMed: 2339632]

[19]. Wei W, Pang S, Sun D, The pathogenesis of endemic fluorosis: Research progress in the last 5 years, J Cell Mol Med 23(4) (2019) 2333–2342. [PubMed: 30784186]

[20]. Fina BL, Lupo M, Da Ros ER, Lombarte M, Rigalli A, Bone Strength in Growing Rats Treated with Fluoride: a Multi-dose Histomorphometric, Biomechanical and Densitometric Study, Biol Trace Elem Res 185(2) (2018) 375–383. [PubMed: 29396777]

[21]. Simon M, Beil F, Rüther W, Busse B, Koehne T, Steiner M, Pogoda P, Ignatius A, Amling M, Oheim R, High fluoride and low calcium levels in drinking water is associated with low bone mass, reduced bone quality and fragility fractures in sheep, Osteoporos Int 25(7) (2014) 1891–1903. [PubMed: 24777741]

[22]. Turner C, Garetto L, Dunipace A, Zhang W, Wilson M, Grynpas M, Chachra D, McClintock R, Peacock M, Stookey G, Fluoride treatment increased serum IGF-1, bone turnover, and bone mass, but not bone strength, in rabbits, Calcif Tissue Int 61(1) (1997) 77–83. [PubMed: 9192519]

[23]. Silva MJ, Ulrich SR, In vitro sodium fluoride exposure decreases torsional and bending strength and increases ductility of mouse femora, J Biomech 33(2) (2000) 231–4. [PubMed: 10653038]

[24]. Rinnerthaler S, Roschger P, Jakob HF, Nader A, Klaushofer K, Fratzl P, Scanning small angle X-ray scattering analysis of human bone sections, Calcif Tissue Int 64(5) (1999) 422–9. [PubMed: 10203419]

[25]. Roschger P, Fratzl P, Klaushofer K, Rodan G, Mineralization of cancellous bone after alendronate and sodium fluoride treatment: a quantitative backscattered electron imaging study on minipig ribs, Bone 20(5) (1997) 393–7. [PubMed: 9145235]

[26]. Fratzl P, Schreiber S, Roschger P, Lafage MH, Rodan G, Klaushofer K, Effects of sodium fluoride and alendronate on the bone mineral in minipigs: a small-angle X-ray scattering and backscattered electron imaging study, J Bone Miner Res 11(2) (1996) 248–53. [PubMed: 8822349]

[27]. Fratzl P, Roschger P, Eschberger J, Abendroth B, Klaushofer K, Abnormal bone mineralization after fluoride treatment in osteoporosis: a small-angle x-ray-scattering study, J Bone Miner Res 9(10) (1994) 1541–9. [PubMed: 7817799]

[28]. Bouxsein ML, Determinants of skeletal fragility, Best Pract Res Clin Rheumatol 19(6) (2005) 897–911. [PubMed: 16301186]

[29]. Burket JC, Brooks DJ, MacLeay JM, Baker SP, Boskey AL, van der Meulen MC, Variations in nanomechanical properties and tissue composition within trabeculae from an ovine model of osteoporosis and treatment, Bone 52(1) (2013) 326–36. [PubMed: 23092698]

[30]. Donnelly E, Chen DX, Boskey AL, Baker SP, van der Meulen MC, Contribution of mineral to bone structural behavior and tissue mechanical properties, Calcif Tissue Int 87(5) (2010) 450–460. [PubMed: 20730582]

[31]. Akkus O, Adar F, Schaffler MB, Age-related changes in physicochemical properties of mineral crystals are related to impaired mechanical function of cortical bone, Bone 34(3) (2004) 443–53. [PubMed: 15003792]

[32]. Burr DB, The contribution of the organic matrix to bone's material properties, Bone 31(1) (2002) 8–11. [PubMed: 12110405]

[33]. Burstein AH, Zika JM, Heiple KG, Klein L, Contribution of collagen and mineral to the elastic-plastic properties of bone., J Bone Joint Surg Am 57(7) (1975) 956–61. [PubMed: 1184645]

[34]. Güerri-Fernández RC, Nogués X, Quesada Gómez JM, Torres del Pliego E, Puig L, García-Giralt N, Yoskovitz G, Mellibovsky L, Hansma PK, Díez-Pérez A, Microindentation for in vivo measurement of bone tissue material properties in atypical femoral fracture patients and controls, J Bone Miner Res 28(1) (2013) 162–168. [PubMed: 22887720]

[35]. Jenkins T, Katsamenis O, Andriotis O, Coutts L, Carter B, Dunlop D, Oreffo R, Cooper C, Harvey N, Thurner P, The inferomedial femoral neck is compromised by age but not disease: Fracture toughness and the multifactorial mechanisms comprising reference point microindentation, J Mech Behav Biomed Mat 75 (2017) 399–412.

[36]. Abraham AC, Agarwalla A, Yadavalli A, McAndrew C, Liu JY, Tang SY, Multiscale predictors of femoral neck in situ strength in aging women: contributions of BMD, cortical porosity, reference point indentation, and nonenzymatic glycation, J Bone Miner Res 30(12) (2015) 2207–2214. [PubMed: 26060094]

[37]. Diez-Perez A, Güerri R, Nogues X, Cáceres E, Peña MJ, Mellibovsky L, Randall C, Bridges D, Weaver JC, Proctor A, Microindentation for in vivo measurement of bone tissue mechanical properties in humans, J Bone Miner Res 25(8) (2010) 1877–1885. [PubMed: 20200991]

[38]. Karim L, Moulton J, Van Vliet M, Velie K, Robbins A, Malekipour F, Abdeen A, Ayres D, Bouxsein ML, Bone microarchitecture, biomechanical properties, and advanced glycation end-products in the proximal femur of adults with type 2 diabetes, Bone 114 (2018) 32–39. [PubMed: 29857063]

[39]. Gallant MA, Brown DM, Organ JM, Allen MR, Burr DB, Reference-point indentation correlates with bone toughness assessed using whole-bone traditional mechanical testing, Bone 53(1) (2013) 301–305. [PubMed: 23274349]

[40]. Hansma P, Turner P, Drake B, Yurtsev E, Proctor A, Mathews P, Lulejian J, Randall C, Adams J, Jungmann R, Garza-de-Leon F, Fantner G, Mkrtchyan H, Pontin M, Weaver A, Brown MB, Sahar N, Rossello R, Kohn D, The bone diagnostic instrument II: indentation distance increase, Rev Sci Instrum 79(6) (2008) 064303. [PubMed: 18601422]

[41]. Hansma P, Yu H, Schultz D, Rodriguez A, Yurtsev EA, Orr J, Tang S, Miller J, Wallace J, Zok F, Li C, Souza R, Proctor A, Brimer D, Nogues-Solan X, Mellbovsky L, Pena MJ, Diez-Ferrer O, Mathews P, Randall C, Kuo A, Chen C, Peters M, Kohn D, Buckley J, Li X, Pruitt L, Diez-Perez A, Alliston T, Weaver V, Lotz J, The tissue diagnostic instrument, Rev Sci Instrum 80(5) (2009) 054303. [PubMed: 19485522]

[42]. Vashishth D, Gibson GJ, Khoury JI, Schaffler MB, Kimura J, Fyhrie DP, Influence of nonenzymatic glycation on biomechanical properties of cortical bone., Bone 28(2) (2001) 195–201. [PubMed: 11182378]

[43]. Silva MJ, Ulrich SR, In vitro sodium fluoride exposure decreases torsional and bending strength and increases ductility of mouse femora, J Biomech 33(2) (2000) 231–234. [PubMed: 10653038]

[44]. Compston JE, Chadha S, Merrett AL, Osteomalacia developing during treatment of osteoporosis with sodium fluoride and vitamin D., Br Med J 281(6245) (1980) 910–1. [PubMed: 7427505]

[45]. Turner CH, Owan I, Brizendine EJ, Zhang W, Wilson ME, Dunipace AJ, High fluoride intakes cause osteomalacia and diminished bone strength in rats with renal deficiency., Bone 19(6) (1996) 595–601. [PubMed: 8968025]

[46]. DePaula CA, Abjornson C, Pan Y, Kotha SP, Koike K, Guzelsu N, Changing the structurally effective mineral content of bone with in vitro fluoride treatment, J Biomech 35(3) (2002) 355–61. [PubMed: 11858811]

[47]. Reid IR, Cundy T, Grey AB, Horne A, Clearwater J, Ames R, Orr-Walker BJ, Wu F, Evans MC, Gamble GD, King A, Addition of monofluorophosphate to estrogen therapy in postmenopausal osteoporosis: a randomized controlled trial., J Clin Endocrinol Metab 92(7) (2007) 2446–52. [PubMed: 17440020]

[48]. Gupta R, Kumar A, Bandhu S, Gupta S, Skeletal fluorosis mimicking seronegative arthritis, Scan J Rheumatol 36(2) (2007) 154–155.

[49]. Hammond MA, Gallant MA, Burr DB, Wallace JM, Nanoscale changes in collagen are reflected in physical and mechanical properties of bone at the microscale in diabetic rats, Bone 60C (2013) 26–32.

[50]. Grynpas M, Age and disease-related changes in the mineral of bone, Calcif Tissue Int 53 Suppl 1 (1993) S57–64. [PubMed: 8275381]

[51]. Grynpas MD, Rey C, The effect of fluoride treatment on bone mineral crystals in the rat, Bone 13(6) (1992) 423–9. [PubMed: 1476820]

[52]. Evans FG, Wood JL, Mechanical properties and density of bone in a case of severe endemic fluorosis, Acta Orthop Scand 47(5) (1976) 489–495. [PubMed: 998183]

[53]. Alarcon-Herrera MT, MartIn-Dominguez IR, Trejo-Vázquez R, Rodriguez-Dozal S, Well water fluoride, dental fluorosis, and bone fractures in the Guadiana Valley of Mexico, Fluoride 34(2) (2001) 139–149.

[54]. Haettich B, Lebreton C, Prier A, Kaplan G, Magnetic resonance imaging of fluorosis and stress fractures due to fluoride, Revue du rhumatisme et des maladies osteo-articulaires 58(11) (1991) 803–808. [PubMed: 1780657]

[55]. Boivin G, Chavassieux P, Chapuy M, Baud C, Meunier P, Skeletal fluorosis: histomorphometric analysis of bone changes and bone fluoride content in 29 patients, Bone 10(2) (1989) 89–99. [PubMed: 2765315]

[56]. Littleton J, Paleopathology of skeletal fluorosis, Am J Phys Anthropol 109(4) (1999) 465–483. [PubMed: 10423263]

[57]. Nelson EA, Halling CL, Buikstra JE, Evidence of Skeletal Fluorosis at the Ray Site, Illinois, USA: a pathological assessment and discussion of environmental factors, Int J Pathopaleo 26 (2019) 48–60.

[58]. Petrone P, Giordano M, Giustino S, Guarino FM, Enduring fluoride health hazard for the Vesuvius area population: the case of AD 79 Herculaneum, PloS one 6(6) (2011) e21085. [PubMed: 21698155]

[59]. Boussouga Y-A, Valentukeviciene M, Zurauskiene R, Research on Fluoride Removal from Membranes Rejected Water, Environmental Engineering. Proceedings of the International Conference on Environmental Engineering. ICEE, Vilnius Gediminas Technical University, Department of Construction Economics, 2017, pp. 1–6.

[60]. Petrone P, Guarino FM, Giustino S, Gombos F, Ancient and recent evidence of endemic fluorosis in the Naples area, J Geochem Explor 131 (2013) 14–27.

[61]. Jacobsen SJ, Goldberg J, Cooper C, Lockwood SA, The association between water fluoridation and hip fracture among white women and men aged 65 years and older: a national ecologic study, Ann Epidemiol 2(5) (1992) 617–626. [PubMed: 1342313]

[62]. Danielson C, Lyon JL, Egger M, Goodenough GK, Hip fractures and fluoridation in Utah's elderly population, JAMA 268(6) (1992) 746–748. [PubMed: 1640574]

[63]. Simonen O, Laitinen O, Does fluoridation of drinking-water prevent bone fragility and osteoporosis?, Lancet 326(8452) (1985) 432–434.

[64]. Giavaresi G, Fini M, Gnudi S, Mongiorgi R, Ripamonti C, Zati A, Giardino R, The mechanical properties of fluoride-treated bone in the ovariectomized rat, Calcif Tissue Int 65(3) (1999) 237–41. [PubMed: 10441658]

[65]. Karim L, Van Vliet M, Bouxsein ML, Comparison of cyclic and impact-based reference point indentation measurements in human cadaveric tibia, Bone 106 (2018) 90–95. [PubMed: 25862290]

[66]. Granke M, Coulmier A, Uppuganti S, Gaddy JA, Does MD, Nyman JS, Insights into reference point indentation involving human cortical bone: sensitivity to tissue anisotropy and mechanical behavior, J Mech Behav Biomed Mat 37 (2014) 174–85.

Highlights

- High fluoride increases indentation distances and lowers elastic modulus and ultimate stress.
- cRPI indentation distances were inversely related to elastic modulus and ultimate stress.
- In vitro NaF incubation detrimentally affects bone's mechanical behavior.

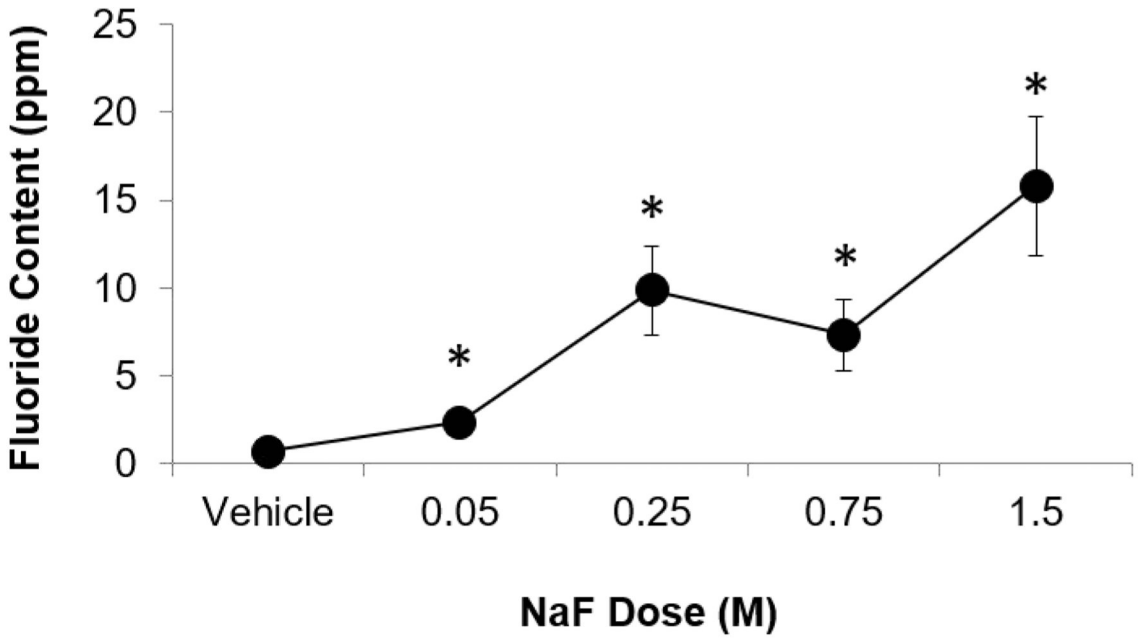

Figure 1. Measured bone fluoride content vs NaF concentration.

Bone fluoride content increased with increasing NaF concentration. Asterisk denotes that the average value of the group is significantly greater than of the vehicle group ($p \leq 0.05$).

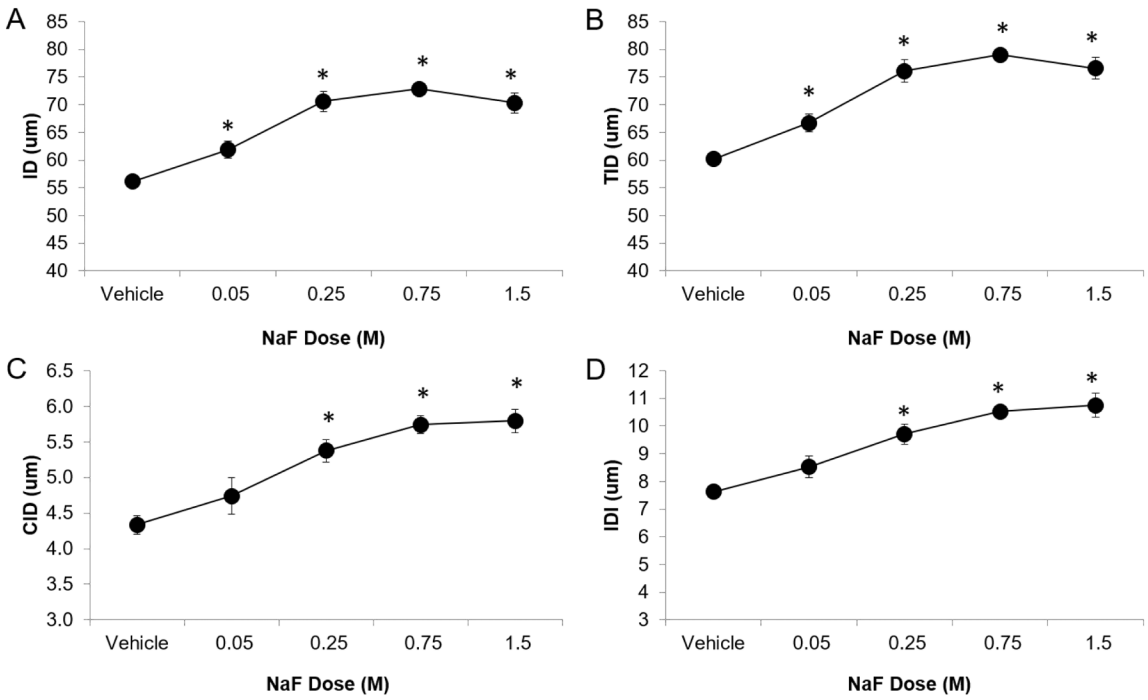

Figure 2. cRPI-assessed indentation distances vs NaF concentration.

Indentation distances increased with increasing NaF concentration. Asterisk denotes that the average value of the group is significantly greater than of the vehicle group ($p \leq 0.05$).

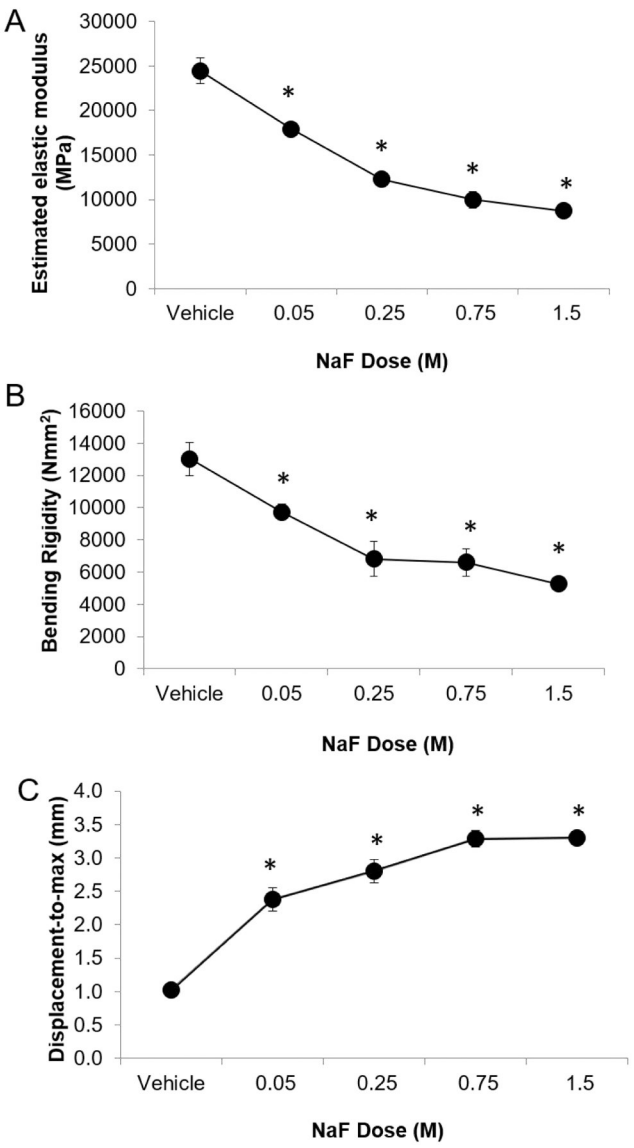

Figure 3. Whole bone biomechanical properties vs NaF concentration.

Whole bone stiffness, estimated elastic modulus, and bending rigidity all decreased while displacement-to-maximum increased with increasing NaF concentration. Asterisk denotes that the average value of the group is significantly greater than of the vehicle group ($p \leq 0.05$).

Bone. Author manuscript; available in PMC 2021 July 01.

Table 1.

Summary of bone geometry, tissue mineral density, cRPI variables, and whole bone biomechanical properties of NaF-incubated and vehicle control bones. Values are reported as average ± standard deviation for each group. Groups shaded in grey are significantly different from the vehicle group ($p \leq 0.05$).

	Properties	Vehicle	0.05M NaF	0.25M NaF	0.75M NaF	1.5M NaF
MicroCT	I_{max} (mm^4)	0.52±0.08	0.56±0.07	0.55±0.18	0.65±0.10	0.61±0.10
	I_{min} (mm^4)	0.08±0.01	0.08±0.01	0.10±0.04	0.09±0.01	0.09±0.02
	Cortical Thickness (mm)	0.64±0.04	0.63±0.03	0.62±0.06	0.65±0.04	0.63±0.03
	Cortical Porosity (%)	0.40±0.19	0.35±0.11	1.55±2.62	0.57±0.32	0.57±0.39
	Cortical TMD (mgHA/ccm)	1103±45	1102±14	1082±41	1075±35	1058±16
cRPI	IDI (μm)	7.63±0.42	8.52±1.16	9.71±1.05	10.52±0.58	10.75±1.24
	ID (μm)	56.1±1.8	61.9±4.5	70.6±5.2	72.8±2.3	70.3±2.2
	TID (μm)	60.2±2.0	66.7±4.9	76.1±5.6	79.0±2.4	76.6±5.6
	CID (μm)	4.33±0.36	4.74±1.76	5.38±0.45	5.74±0.36	5.79±0.47
	Avg CID (μm)	1.58±0.24	1.74±0.32	2.04±0.12	2.04±0.11	2.13±0.25
	Avg ED (μJ)	26.1±1.5	27.2±4.2	32.5±3.2	34.6±3.2	35.1±5.7
	Avg US (N/μm)	0.73±0.03	0.75±0.05	0.73±0.05	0.71±0.04	0.70±0.03
	Avg LS (N/μm)	0.55±0.02	0.57±0.04	0.52±0.04	0.50±0.03	0.50±0.04
3-poing bending	Estimated Elastic Modulus (GPa)	24.5±4.1	17.9±1.8	12.3±2.3	10.0±2.7	8.7±1.5
	Bending Rigidity (Nmm^2)	13,024±2880	9733±1507	6825±3094	6597±2530	5260±971
	Ultimate Moment (Nmm)	24.5±3.1	17.2±4.1	14.3±4.7	11.8±2.2	10.6±1.1
	Ultimate Stress (N/mm^2)	6.62±0.65	4.49±0.91	3.62±1.14	2.83±0.51	2.66±0.0.28
	Work-to-ultimate point (Nmm)	6.5±1.5	13.4±3.9	13.2±4.0	12.8±1.4	11.7±1.0
	Displacement-to-maximum force (mm)	1.02±0.23	2.38±0.53	2.81±0.49	3.28±0.37	3.30±0.20
Fluoride measurement	F^{-} (ppm)	0.70±0.46	2.36±1.73	9.86±6.72	7.31±6.07	15.80±11.29

Table 2.

Correlation coefficients between F^- content, key microCT parameters, cRPI variables, and whole bone biomechanical properties. Significant correlations ($p \leq 0.05$) are shaded in grey.

	MicroCT			3-point bending						Fluoride measurement
	Cortical Thickness (mm)	Cortical Porosity (%)	Cortical TMD (mgHA/ccm)	Estimated Elastic Modulus (GPa)	Bending Rigidity (Nmm^2)	Ultimate Moment (Nmm)	Ultimate Stress (N/mm^2)	Work-to-ultimate point (Nmm)	Displacement-to-maximum force (mm)	F^- (ppm)
cRPI										
IDI (μm)	+0.03	+0.34	−0.30[§]	−0.70	−0.60	−0.57	−0.60	+0.45	+0.64	+0.62
ID (μm)	+0.16	+0.31	−0.28	−0.72	−0.60	−.65	−0.65	+0.50	+0.64	+0.51
TID (μm)	+0.13	+0.33	−0.27	−0.73	−0.61	−0.65	−0.65	+0.52	+0.64	+0.53
CID (μm)	+0.13	+0.23	−0.31	−0.68	−0.56	−0.57	−0.60	+0.40	+0.62	+0.52
Avg CID (μm)	−0.01	+0.24	−0.21	−0.61	−0.46	−0.56	−0.56	+0.53	+0.60	+0.52
Avg ED (μJ)	+0.04	+0.34	−0.41	−0.63	−0.55	−0.61	−0.57	+0.26	+0.57	+0.52
Avg US (N/μm)	+0.12	−0.27	+0.29[§]	+0.32	+0.24	+0.22	+0.19	−0.02	−0.17	−0.27
Avg LS (N/μm)	+0.08	−0.38	+0.38	+0.53	+0.48	+0.47	+0.44	−0.14	−0.41	−0.56
Fluoride measurement										
F^- (ppm)	+0.20	−0.48	−0.030	−0.62	−0.59	−0.59	−0.60	+0.30	+0.60	--

[§] $0.051 \leq p \leq 0.058$